Interpolation methodologies comparison for Heat Index Assessment

Ivone G. Zapata-Wah[1*], Dariela A. Vazquez-Rodriguez[1], Fabiola D. Yepez-Rincon[1], Andrea N. Escobedo-Tamez [1]

[1] Autonomous University of Nuevo Leon, Civil Engineering Institute, Geomatics Department, Mexico, Av. Universidad s/n, Anáhuac, C.P. 66455, San Nicolás de los Garza.

Keywords: heat index, IDW, Kriging, Spline, interpolation, remote sensing

Abstract

Urban development is often accompanied by anthropogenic activities, changes in land morphology and serious damage to natural areas. Consequently, the urban climate is also affected, as temperatures are higher in urban centers and because of the presence of the urban heat island phenomenon, which poses a health threat to local citizens. The Monterrey Metropolitan Area (MMA) is the second-largest urban area in Mexico and is characterized for rapid urbanization and industrialization processes, steep climate conditions and the presence of urban heat islands. This combination makes living conditions rough for its inhabitants, especially for vulnerable groups. In order to quantify and compare heat vulnerability in urban areas, metrics such as the Heat Index measure the heat exposure and its effects on the human body. This study interpolated both relative humidity and temperature information from 15 local climate monitoring stations to determine the Heat Index for the six hottest weeks of the 2023 summer in the Monterrey Metropolitan Area. The interpolation methodologies used (IDW, Kriging and Spline) were later compared in order to cross-validate the results and define the most accurate performance based on both MAE and RMSE statistical analysis.

1. Introduction

Temperatures worldwide have seen an increase in the past decades, as during the period between 1970 and 2020 global temperatures rose by 0.28°C (Silberstein, M.; 2024). This has become a problem specially for urbanized areas. Factors such as anthropogenic heat, a continuous growing population and the presence of urban heat islands (UHI) are a constant challenge for city planners and health officials (Tian, 2023) as the impacts of climate change worsen.

Higher temperatures correlate with higher urbanization rates in the long run (Helbling, M. & Meierrieks, D.; 2023) and, in general, the complex UHI amplification effects are responsible for the local thermal and related UHI global warming forcing issues (Feinberg, A.; 2020). According to Hu et al., (2023), Liu et al., (2023) and García et al., (2022), urbanized areas often experience higher heat wave risk and more severe UHI effects, which are further exacerbated during extreme heat events.

The active development of cities, changes in the urban infrastructure morphology and land use, and anthropogenic activities impose a great influence on the local climate changes of urban areas (Chen, S., Bao, Z., Ou, Y., Chen, K., 2023) and endanger local citizens. People living with extreme UHI conditions are vulnerable to chronic temperature-related diseases (Abbassi, et al., 2023). Research that addresses health effects of weather-related heat exposure is critical both to limit present-day dangers from heat and also to prepare for future weather (Anderson et al., 2013).

According to Xu et al (2025), early studies on urban thermal environments relied primarily on temperature data. However, advances in remote sensing satellite technology for the behavioral evaluation of urban heat islands has become a common approach, as it offers spatial and temporal coverage of the study areas and allows identification of hot spots, supporting urban planning and public health interventions (Shi et al., 2021; Diem et al., 2023). By leveraging satellite and aerial data, monitoring the land surface temperature (LST) and other related indicators to assess the UHI effect can be followed through.

In order to estimate the effect of heat on the human body and the risk of heat stress that the population faces, a number of different indices based on weather variables including air temperature, humidity, solar radiation and wind have been developed (Baldwin et al., 2023). Instruments such as the Heat Index metric (HI) -used to measure human heat stress from temperature and relative humidity data- are among the most temperature-sensitive metrics according to sensitivity analyses (Rachid and Qureshi, 2023) and have proven useful in research endeavors aimed at estimating future changes associated with global climate change (Lanzante, 2024).

For the further evaluation of the Heat Index in urban areas and ensuring data reliability, the air temperature and relative humidity information can be obtained from climate monitoring systems to cover larger cities or urban areas. For the Monterrey Metropolitan Area (MMA), the monitoring stations located in the urban expanse are key to determine the Heat Index present, emphasizing its importance during extreme heat conditions and the summer period. The MMA has expanded rapidly in both size and population and, according to Vivideconomics (2022), it is considered one of the hottest cities in Mexico with temperatures 5°C warmer in its built-up urban core.

A downside of climate monitoring systems is the sparse or uneven distribution of its stations across urban areas, making a necessity the use of interpolation methods to generate information that covers cities or metropolitan areas in its entirety. This study aims to make a comparison between three interpolation methodologies (Inverse Distance Weighted, Kriging and Spline) for relative humidity and air temperature information obtained from the Monterrey Metropolitan Area climate monitoring system. Alongside, the resulting Heat Index images for each method will be evaluated to determine their performance and accuracy and then, cross-validated based on both MAE and RMSE statistical analysis. For this, the study period comprehends the six weeks that reported higher temperatures in the MMA during 2023, as the year reported atypical temperatures in the summer months.

2. Study Area

https://doi.org/10.5194/isprs-archives-XLIX-B3-2026-457-2026

Located in northeastern Mexico, the Monterrey Metropolitan Area houses 5.3 million inhabitants in 16 municipalities (Gobierno del Estado de Nuevo León, 2024): Apodaca, Cadereyta Jiménez, El Carmen, Ciénega de Flores, García, San Pedro Garza García, General Escobedo, General Zuazua, Guadalupe, Juárez, Monterrey, Pesquería, Salinas Victoria, San Nicolás de los Garza, Santa Catarina and Santiago. It comprehends a 7440 km2 area, with only 1119 km2 being occupied with urban centres and around 98.6% of the population living in them (CONAPO, 2020).

It is considered Mexico's second-largest urban agglomeration and a major industrial and economic hub, characterized for both rapid urbanization and industrialization processes along with its population growing constantly at a rate of 2.5% as of 2022 (CONAPO, 2020).

The MMA experiences a semi-arid climate with hot summers, mild winters and highly variable precipitation (González-Hernández, 2019). Aspects such as rapid urbanization, anthropogenic heat and industrial activities and climate change have deepened the environmental challenges in Monterrey and are a direct cause for the intensified local heat. Average annual temperatures are around 25°C, with summer highs often exceeding 30°C and reaching up to 44°C during heatwaves (Magaña, et al., 2021). Moreover, the National Meteorological Service (Servicio Meteorológico Nacional, n.d.) stated that the MMA has a record high of 48°C and daily average temperatures above 28°C for around ten days a year, making its population susceptible to heat stress.

These climate conditions alongside the presence of urban heat islands make living conditions tough. At high temperatures, humans struggle to adjust to their environment and affect their health (Dai and Liu, 2022). Temperatures exceeding the upper tolerance limit may lead to higher mortality rates (Tian et al., 2021) as it was the case for the MMA during 2023, with 102 deaths reported due to extreme heat (DGE, 2023; CENAPRECE, 2024).

2.1 Climate Monitoring System

For the monitoring of environmental conditions, there are several institutions in Mexico responsible for the climate supervision of major cities (Mayora, 2020). The Monterrey Metropolitan Area monitoring system provides essential data for assessing air pollution, temperature and other climate variables since 1992 (Lucia, F.-M. A., and Ulises R.-S. H., 2023).

Consisting of 15 automatic monitoring stations (Table 1, Figure 1), the Integrated Environmental Monitoring System (SIMA for its acronym in Spanish) tracks environmental changes and measures suspended particles, both PM10 and PM2.5 (Lucia, F.-M. A., and Ulises R.-S. H., 2023) by relying on automated stations that register hourly data.

ID	SIMA Station	Municipality
SE	Southeast	Guadalupe
NE	Northeast	San Nicolás de los Garza
CE	Centre	Monterrey
NO	Northwest	Monterrey
SO	Southwest	Santa Catarina
NTE	North	General Escobedo
NO2	Northwest 2	García
NE2	Northeast 2	Apodaca
SE2	Southeast 2	Juárez
SO2	Southwest 2	San Pedro Garza García
SUR	South	Monterrey
NTE2	North 2	San Nicolás de los Garza
SE3	Southeast 3	Cadereyta
NE3	Northeast 3	Pesquería
NO3	Northwest 3	García

Table 1. Climate Monitoring System Stations (Zapata Wah et al., 2026)

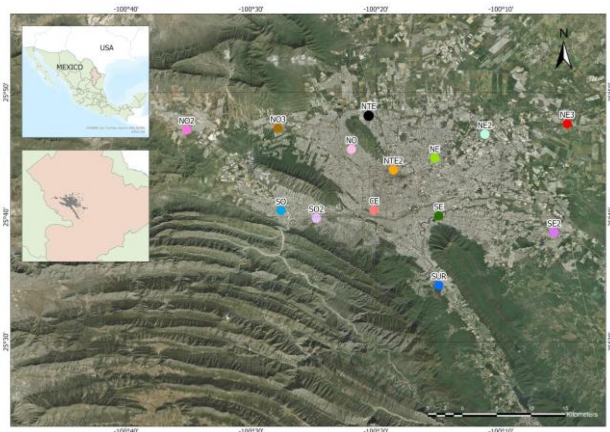

Figure 1. SIMA’s Climate Monitoring Stations across the MMA

3. Materials and Methods

3.1 SIMA Data

The information taken from the SIMA monitoring stations corresponds to 2023, specifically the six weeks with record high mean temperatures, as they reported abnormal increases in temperatures due to heat waves and the overall climate conditions.

The temperature and relative humidity information was divided in three periods of two weeks each over the summer months: summer solstice (24th and 25th weeks), middle of the summer (32nd and 33rd weeks) and close of summer (35th and 36th weeks) (Figure 2).

This contribution has been peer-reviewed.
https://doi.org/10.5194/isprs-archives-XLIX-B3-2026-457-2026

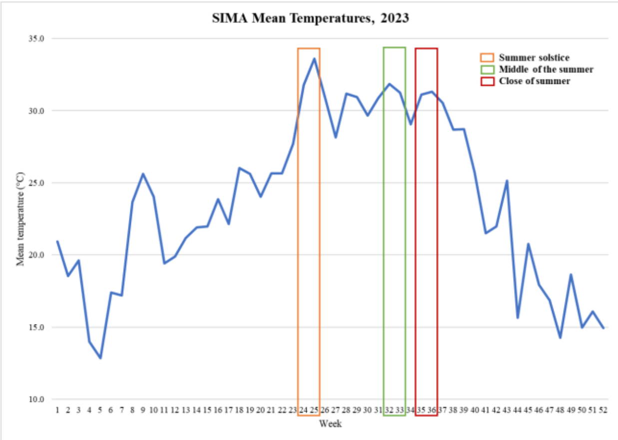

Figure 2. SIMA mean temperatures, 2023

Before the Heat Index calculation, both temperature and relative humidity values were interpolated in order to cover the whole Monterrey Metropolitan Area and not only the climate monitoring stations. This process was essential for the HI estimation across the MMA as the SIMA stations are unevenly distributed.

In order to perform the interpolation analysis mentioned, both relative humidity (RH) and temperature (T) information was converted into weekly mean values as the SIMA stations record information hourly. Three interpolation methods -Inverse Distance Weighted (IDW), Kriging and Spline- were used as the aim is to compare their individual performance.

3.2 Interpolation methods

Spatial interpolation techniques have been successfully introduced into the field of meteorology and climatology, where continuous spatial information on weather or climate is necessary (Szymanowski and Kryza, 2009). The spatialization process is the transformation of point data to extended information from existing geospatial reference data, using interpolation algorithms (Szymanowski and Kryza, 2009).

In order to overcome accuracy limitations from using data from fixed meteorological stations, interpolation methods can be used to estimate variables such as temperature and relative humidity from fixed data (Brabant et al., 2024). For this study, the spatial interpolation methods used were the Inverse Distance Weighted (IDW), Kriging, and Spline. The interpolation methods were applied by using the ArcGIS Pro Spatial Analyst toolbar.

3.2.1 Inverse Distance Weighted

The Inverse Distance Weighted (IDW) is widely applied for spatial interpolation. This deterministic technique estimates values at unsampled locations based on the values and distances of nearby sampled points, following the concept of the distance between queried and measured points increases, the efficiency of the measured point decreases. The IDW method is represented on Equation 1:

$$Z_{x,y} = \frac{\sum_{i=1}^{n} Z_i W_i}{W_i} \tag{1}$$

Where: $Z_{x,y}$ = point to be estimated
Z_i = control value for the i^{th} sample point
W_i = weight assigned to sampling point

The IDW is a simple, low computationally and intensive method considered as one of the standard spatial interpolation methods in geographic information science (Lu and Wong, 2008). Additionally, Karakaya et al., (2016) mention that the IDW is usually applied to highly variable data such as soil chemistry results, consumer behavior observations and environmental monitoring data, as its algorithm is a moving average interpolator.

3.2.2 Kriging

Kriging incorporates the concept of randomness in spatial processes (Szymanowski and Kryza, 2009) and analyses the spatial distribution of variability of the interpolated variable. It is a local interpolation method that uses a subset of geostatistical interpolation methods (Hadi, 2018).

This technique assumes that closer points are more likely to be similar, and farther points are more likely to be different. Ozelkan (2015), mention that Kriging is a variant of the basic linear regression estimator and it is defined as Equation 2:

$$Z(u) - m(u) = \sum_{i=1}^{n} \lambda_i [Z(u_i) - m(u_i)] \tag{2}$$

Where: $Z(u)$ = is the estimated value
$Z(u_i)$ = measurement at location
λ_i = assigned weights to measurements
u = location
$m(u)$, $m(u_i)$ = means of $Z(u)$ and $Z(u_i)$
N = number of measurements

3.2.3 Spline

The Spline is an interpolation method that uses functions to approximate surfaces. Spline is categorized into the functions, the regular and the tensile. The regular method uses values that could be possible outside the range of the data sample to create a smooth gradient surface. While the tensile method uses the characteristics of the modeled phenomenon to control the hardness of the surface (Feng, 2024).

The surface interpolation $S(x,y)$, of the Spline method is expressed as shown in Equation 3:

$$S(x,y) = T(x,y) + \sum_{i=1}^{n} \lambda_i R(r_j) \quad j = 1,2 \ldots N \tag{3}$$

Where: N = number of points
λ_i = coefficient by the solving system of linear equations
T(x,y) = used in tensile method
(r_j) = used in the regular method.

For this research we used specifically the Regular method, to obtain R(r) as demonstrated in Equation 4:

$$R(r) = \frac{1}{2}\pi\left(r\frac{2}{4} + t^2\left[K0\left(\frac{r}{t}\right) + c + ln\left(\frac{r}{2\pi}\right)\right]\right) \tag{4}$$

Where: r = distances between sample and point
p^2 = weight parameter
K0 = modified Bassel function.
c = constant equal to 0.577215

Regular splines produce smoother interpolations than tensile splines. Moreover, when using the regular spline method, increasing the smoothing weight results in a progressively smoother interpolated surface.

3.3 Cross-Validation Statistics

To establish a robust quantitative validation framework, ground-based observations were compared with the interpolated temperature and relative humidity datasets through statistical analysis.

3.3.1 MAE and RMSE

The mean absolute error (MAE) was used to quantify the average magnitude of errors, assigning equal weight to all deviations (Equation 5). In contrast, the root means square error (RMSE) was employed to emphasize larger errors, as it is more sensitive to extreme values and influenced by outliers (Equation 5 and 6).

$$MAE = \frac{1}{n}\sum_{i=1}^{n}(X_i - Y_i) \tag{5}$$

$$RMSE = \sqrt{\frac{1}{n}\sum_{i=1}^{n}(X_i - Y_i)^2} \tag{6}$$

Where: X_i = the variable X_i denotes estimated values
Y_i = the volume of observed values
n = occurrence

In both metrics, the ideal value is 0, indicating a perfect match between observed and estimated values. However, the magnitude of the results is influenced by the scale of the variable being analyzed, meaning that larger values in the dataset can lead to higher error values (Willmott & Matsuura, 2005).

3.4 Heat Index

The Heat Index (HI) metric provides a means of quantifying and comparing absolute heat vulnerability across different neighborhoods (Kamath et al.,2023) by measuring the heat exposure and its effects on the human body.

Grounded on ambient temperature and relative humidity, the HI is based on a model of human thermoregulation in which each value maps onto a unique state of the human body. The United States National Weather Service has linked these values to environmental health threats (Figure 3) (Romps and Lu, 2023; Anderson, 2013). It has found wide applicability for estimating human heat stress and has proven useful in research aimed at estimating future changes associated with global climate change (Lanzante, 2024).

The HI health threat values are divided in 5 categories -safe, caution, extreme caution, danger and extreme danger- that indicate the risk of heat stress according to specific Heat Index values, as well as the health impacts caused by prolonged exposure to heat (Table 2). HI values in the safe category are the ones with temperatures below 26°C and with no adverse effects related to heat exposure. Temperatures between the 27°C and 41°C marks indicate caution and extreme caution respectively, while readings over 41°C mean danger.

Temperature)°C) \ Relative Humidity (%)	10	20	30	40	50	60	70	80	90
26	25	25	26	26	27	27	28	28	28
27	26	26	26	27	27	28	29	30	31
28	27	27	27	28	28	29	31	32	34
29	27	27	28	30	30	31	33	35	37
30	28	28	29	30	31	33	35	38	41
31	29	29	30	31	33	35	38	41	45
32	30	30	31	32	34	37	40	44	49
33	31	31	32	34	36	40	43	48	54
34	31	32	33	35	38	42	47	52	>52
35	32	33	35	37	41	45	50	>52	>52
36	33	34	36	39	43	49	>52	>52	>52
37	34	35	38	41	46	51	>52	>52	>52
38	35	37	39	43	49	>52	>52	>52	>52
39	36	38	41	46	52	>52	>52	>52	>52
40	37	39	43	48	>52	>52	>52	>52	>52
41	38	41	45	51	>52	>52	>52	>52	>52
42	39	42	47	52	>52	>52	>52	>52	>52
43	40	44	49	>52	>52	>52	>52	>52	>52
44	41	46	52	>52	>52	>52	>52	>52	>52
45	42	47	>52	>52	>52	>52	>52	>52	>52
46	43	49	>52	>52	>52	>52	>52	>52	>52
47	44	51	>52	>52	>52	>52	>52	>52	>52
48	45	52	>52	>52	>52	>52	>52	>52	>52
49	47	>52	>52	>52	>52	>52	>52	>52	>52
50	48	>52	>52	>52	>52	>52	>52	>52	>52

Figure 3. Heat Index health threat values (US Department of Commerce, N.; 2024)

Warning	Heat Index	Health impact
Safe	< 26 °C	No adverse effects expected due to heat
Caution	27 - 32 °C	Fatigue possible with prolonged exposure and/or physical activity
Extreme Caution	32 - 41 °C	Sunstroke, muscle cramps, and/or heat exhaustion possible with prolonged exposure and/or physical activity.
Danger	41 - 52 °C	Sunstroke, heat cramps or heat exhaustion likely possible with prolonged exposure and/or physical activity
Extreme Danger	52 °C or higher	Heat stroke or sunstroke highly likely

Table 2. Danger levels associated with the Heat Index (US Department of Commerce, N. 2024.)

For this study, the Heat Index was calculated for the three interpolation methodologies using the Heat Index function in ArcGIS Pro. The raster analysis uses the following equation to calculate the apparent temperature based on ambient temperature and relative humidity:

$$\begin{aligned} Heat\ Index = {} & (-42.379 + (2.04901523T) \\ & + (10.14333127R) - (0.2247554TR) \\ & - (6.83783e^{-3}TT) - (5.481717e^{-2}R) \end{aligned} \tag{7}$$

$$+ (1.22894e^{-3}TTR) + (8.5282e^{-4}TTR) - (1.99e^{-6}TTRR)$$

Where: T = air temperature
R = relative humidity

4. Results

4.1 Relative Humidity

The three interpolation methods were applied for the 6 study weeks (Figure 4). A notorious characteristic was that the IDW and Kriging methodologies presented similar scope values as opposed to the Spline interpolation method, which used larger humidity ranges for all the study weeks.

In the case of the summer solstice weeks (24th and 25th) the difficulty to identify the SIMA stations or interpolation points varies per method. For the IDW the sampling points are easily identifiable, while for the Kriging and Spline methodologies it was harder. This is also appreciated in the following middle and close of the summer periods (32nd, 33rd weeks and 35th, 36th weeks).

A Spline method characteristic that was visible for the whole study period is that the interpolation has a radius-like behavior with lower humidity levels concentrated in the center. The humidity percentage then exponentially grows towards the outskirts of the study area.

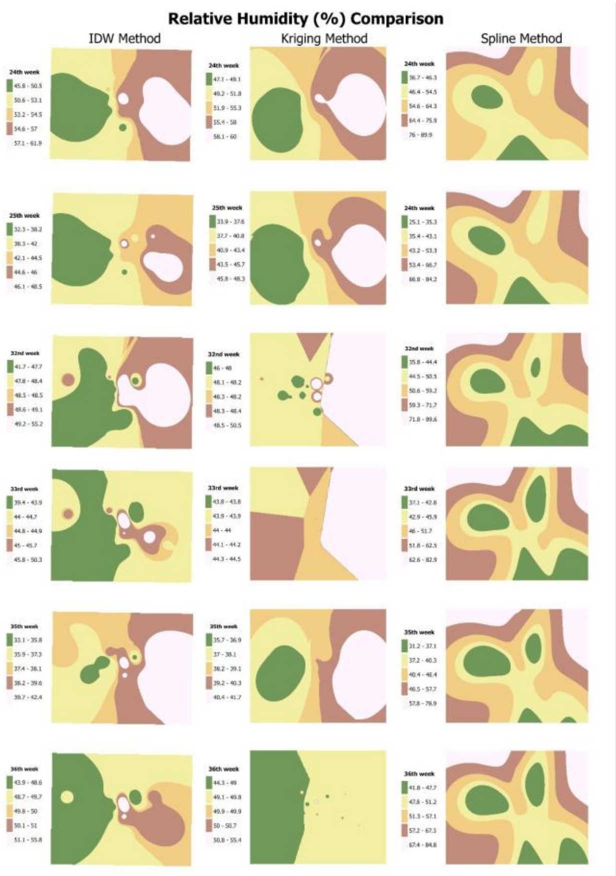

Figure 4. Relative humidity obtained by applied IDW, Kriging and Spline interpolation methods.

4.2 Temperature

Three interpolation methods are used to provide an interpolated temperature map for the study area based on measured points. The interpolation methods obtained similar values over the same areas. The IDW and Kriging have similar range values, while Spline obtained ranges with more scope. This asset from Spline could imply an overestimation of the temperatures or errors that need to be attached and compared directly to the SIMA Stations.

The temperatures of 25th week showed the highest degrees of the summer season of 2023. It is important to notice, that following on Figure 5 temperatures, the center of the urban area showed the maximum ranges of temperature. Contrary to the observations in the incoming weeks, the west side showed the minimum ranges of temperatures. On the other hand, the east side of the urban areas obtained the highest temperatures in all study weeks except 24th and 25th. This performance is linked to the industrial area of the Monterrey Metropolitan Area.

Following the obtained interpolations, Spline exhibited smoother results while IDW presented more roughness and notable points near to the SIMA stations. This is a characteristic of the method but compared to the other two, the IDW tends to focus but tends to obtain less errors and under or overestimation (Feng, 2024; Hadi and Tombul, 2018).

Qiao (2018) comments that the Kriging method tends to underestimate high values and overestimates lower values. Moreover, Qiao (2018) also explains that a uniform distribution of point controls (stations) could improve the interpolation, instead of increasing the point controls without a specific spatial distribution.

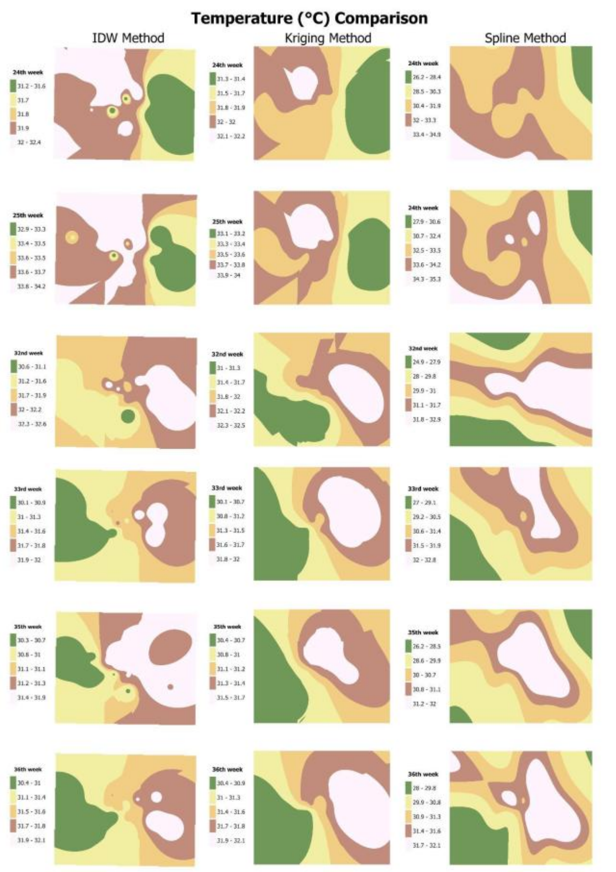

https://doi.org/10.5194/isprs-archives-XLIX-B3-2026-457-2026

Figure 5. Temperatures obtained by applied IDW, Kriging and Spline interpolation methods.

4.3 Statistical Evaluation

Both statistical analyses were applied to the interpolated temperature and relative humidity datasets. For temperature, the results indicate that MAE values range between 0.41 and 0.70, while RMSE values vary from 0.47 to 0.84, suggesting overall good accuracy (Figure 6).

All interpolation methods performed appropriately, obtaining low error values in both metrics. Among them, the Inverse Distance Weighting (IDW) method demonstrated greater consistency across the analyzed weeks and produced the lowest RMSE values, followed by the Kriging method. In contrast, the Spline method was less reliable, as it consistently exhibited higher error values, this performance aligned with previous studies where temperatures were interpolated (Feng, 2024, Hadi, 2018).

In the case of relative humidity (Figure 7), the errors are notably higher than those obtained for temperature, similar to those obtained by Ozelkan (2015). MAE values ranging from 4.0 to 20.0 indicate greater variability and increased difficulty in accurately interpolating humidity. Additionally, the higher RMSE values relative to MAE suggest the presence of large individual errors or outliers.

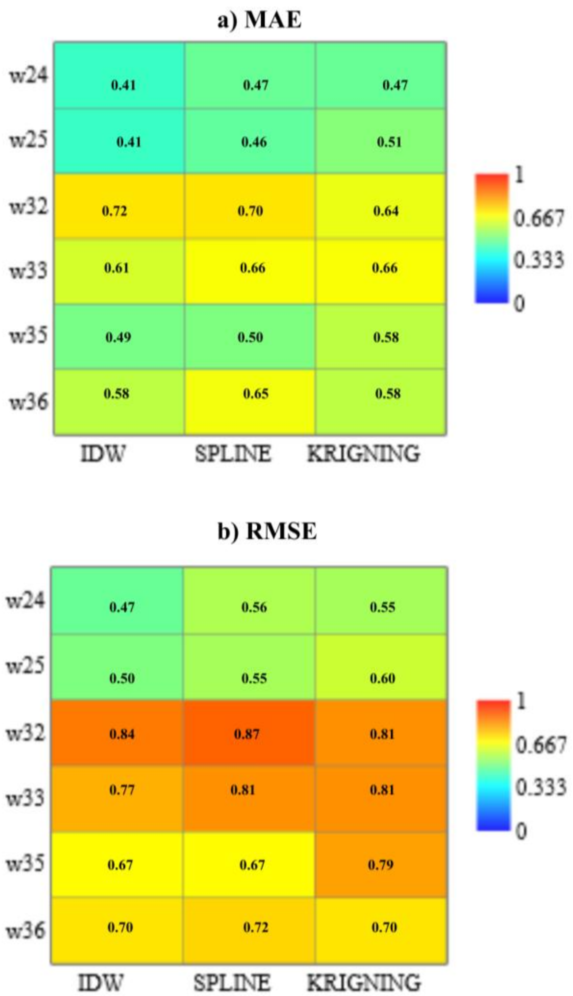

Figure 6. MAE and RMSE for interpolated temperatures

In contrast to the temperature analysis, the Inverse Distance Weighting (IDW) method performed the worst for humidity interpolation, as reflected by consistently higher MAE and RMSE values (Figure 7). Conversely, the Spline and Kriging methods yielded better overall performance. However, the MAE values associated with the Kriging method suggest some instability, likely due to outliers, which is particularly evident in week 36 (Figure 7).

These results appear to be more strongly influenced by the nature of the interpolated variable than by the interpolation method itself. Relative humidity exhibits greater spatial variability and is highly sensitive to local conditions, both in magnitude and distribution. In contrast, temperature tends to vary more smoothly, showing gradual changes in both spatial patterns and values.

Based on these results, an improved estimation of the Heat Index (HI) could be achieved by combining interpolation methods. Specifically, the use of IDW for temperature and either Kriging or Spline for relative humidity is recommended, as this combination is likely to enhance the overall accuracy of HI estimations. This scenario will be discussed in the next section.

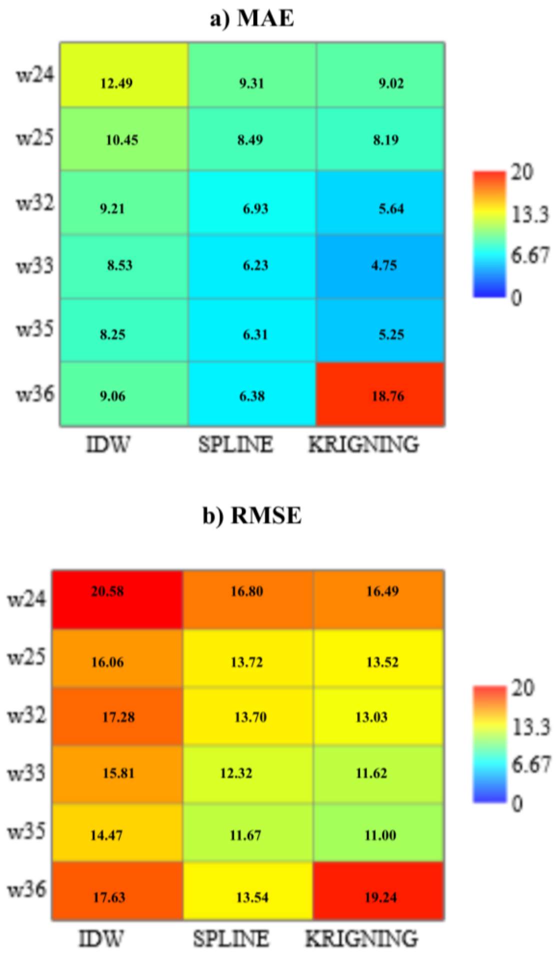

Figure 7. MAE and RMSE for interpolated relative humidity

4.4 Heat Index

The HI interpolations showed consistently elevated values throughout all analyzed weeks. According to the classification presented in Table 2, the Monterrey Metropolitan Area remained predominantly within the "caution" to "extreme caution" categories during the summer of 2023. These results reflect the combined influence of the interpolated temperature and relative humidity fields, which together contribute to increased thermal stress across the region.

The Heat Index obtained from the RH and T Spline interpolation methodology exhibits higher values than those based on IDW and Kriging methods; this performance is linked to the problems in interpolating HR by spline (Figure 7). As observed in Figure 8, the Spline values are overestimated, resulting in HI in the "extreme caution" danger level.

On the other hand, IDW and Kriging showed similar values, with both methodologies having results between 29°C to 34°C on different weeks. Also, for both methods the west side of the MMA (the mountain region) presents lower HI values compared to the urbanized area. It is important to mention that these lower values are around 31°C and are linked to the temperatures reported on Figure 5.

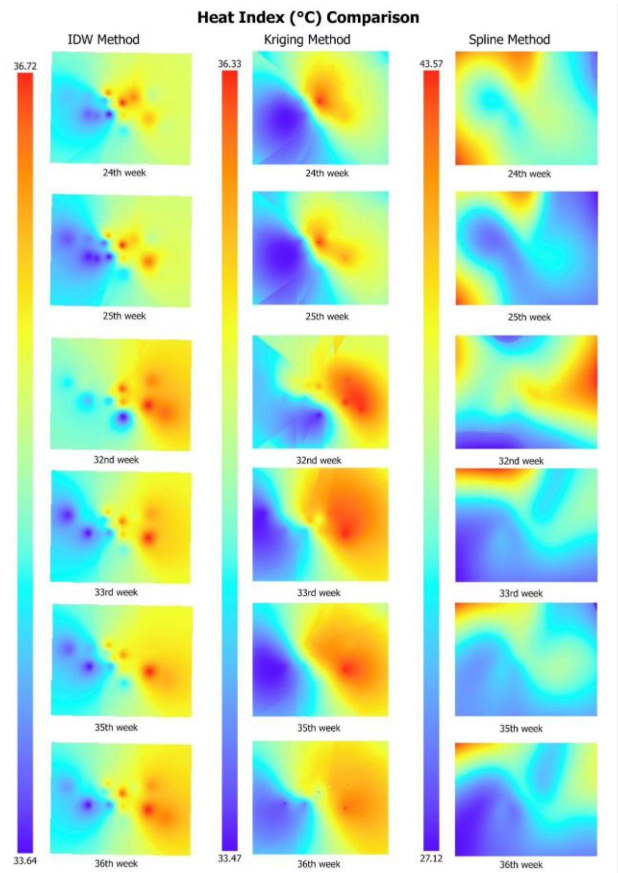

Figure 8. Heat Index obtained by applied IDW, Kriging and Spline interpolation methods.

As reported in Figure 8, the urban heat islands can be distinguished near to Monterrey's industrial zone. This outcome aligns with the findings in the temperature section for the IDW and Kriging assessments, while Spline reflects a more smoothed interpolation.

As discussed in the Statistical Evaluation section, improved Heat Index (HI) estimates can be achieved by combining different interpolation methods. To assess this, two combinations of interpolated temperature and relative humidity were applied to compute HI. Rather than evaluating all six study weeks, the analysis was conducted for a single representative case: week 25, selected due to its high variability in both temperature and relative humidity.

For a first instance, where combined the resulting IDW temperature values alongside Spline for relative humidity (Figure 9, a) to obtain Heat Index. As can be appreciated, the results do not reflect the expected improvement in accuracy, as most of the Monterrey Metropolitan Area presents similar HI values and there are no significant differences in temperature between the urbanized areas and the mountain region.

On the other side, by combined Kriging relative humidity instead Spline (Figure 9, b), the resulting Heat Index coincides with the expected results, as it is possible to appreciate the urban heat islands and the difference in HI values between the urbanized areas, the industrial zones and the mountain region.

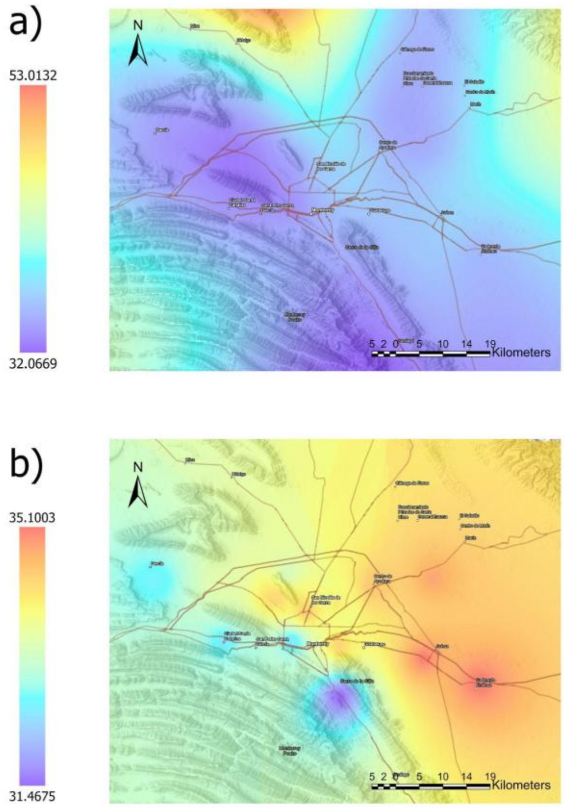

Figure 9. Improved Heat Index for the 25th week. a) Heat Index with IDW for temperature and Spline for relative humidity. b) Heat Index with IDW for temperature and Kriging for relative humidity.

5. Conclusions

The applied interpolation methodologies had an overall well performance and, at a glance, the resulting temperature and relative humidity, alongside the heat index, performed better with the IDW interpolation method.

By applying both MAE and RMSE statistical methods, it was determined that although the temperature variable did perform better with IDW, the relative humidity had better results with Kriging, resulting in an improved Heat Index. This improved HI represented pertinently the heat index behavior in the Monterrey

Metropolitan Area, as it was possible to appreciate the fluctuations between urbanized and natural areas.

It is important to consider that the spatial distribution of the climate monitoring stations can influence the interpolation accuracy. For Monterrey, the SIMA stations were located over time following the growth of the metropolitan area since 1992, resulting in a monitoring network that has not caught up to the newest urbanized areas as of today.

References

Abbassi, Y.; Ahmadikia, H.; Baniasadi, E., 2023: Impact of wind speed on urban heat and pollution islands. Urban Climate, 44, https://doi.org/10.1016/j.uclim.2022.101200.

Anderson, B., Bell, M., and Peng, R., 2013: Methods to Calculate the Heat Index as an Exposure Metric in Environmental Health Research. Environmental Health Perspectives, 121, 1111 - 1119. https://doi.org/10.1289/ehp.1206273.

Baldwin, J. W., T. Benmarhnia, K. L. Ebi, O. Jay, N. J. Lutsko, and J. K. Vanos, 2023: Humidity’s role in heat-related health outcomes: A heated debate. Environ. Health Perspect., 131, 055001, https://doi.org/10.1289/EHP11807.

Brabant, C., Dubreuil, V. and Dufour, S. (2024) Evaluation of spatial interpolation techniques for urban heat island monitoring in small and medium sized cities. Front. Built Environ. 10:1455047. https://doi.org/10.3389/fbuil.2024.1455047

CENAPRECE. (2024). Temporada de Calor, Prevención y Atención de Daños a la Salud, 2024. https://www.gob.mx/cms/uploads/attachment/file/903561/TEMPORADA_DE_CALOR__2024_FINAL__2_.pdf

Chen, S.; Bao, Z.; Ou, Y.; Chen, K., 2023: The synergistic effects of air pollution and urban heat island on public health: A gender-oriented nationwide study of China. Urban Climate, 51, https://doi.org/10.1016/j.uclim.2023.101671.

CONAPO, INEGI, Sedatu., 2020: Metrópolis de México. https://www.gob.mx/sedatu/documentos/metropolis-de-mexico-2020?state=published

Dai Y and Liu T (2022) Spatiotemporal mechanism of urban heat island effects on human health—Evidence from Tianjin city of China. Front. Ecol. Evol. 10:1010400. doi: 10.3389/fevo.2022.1010400

Diem, P., Nguyen, C., Diem, N., Diep, N., Thao, P., Hong, T., and Phan, T., 2023: Remote sensing for urban heat island research: Progress, current issues, and perspectives. *Remote Sensing Applications: Society and Environment*. https://doi.org/10.1016/j.rsase.2023.101081.

DGE, 2023: Temperaturas naturales extremas (Temporada de calor 2023). https://www.gob.mx/cms/uploads/attachment/file/845222/TNE_2023_SE29.pdf

Feinberg, A., 2020: Urban heat island amplification estimates on global warming using an albedo model. SN Appl. Sci. 2, 2178. https://doi.org/10.1007/s42452-020-03889-3

Feng, Z., Wang, R., Liu, X., Huang, M., and Huo, L., 2024: Spatial Interpolation Methods of Temperature Data Based on Geographic Information System—Taking Jiangxi Province as an Example. *Proceedings*, 110(1), 14. https://doi.org/10.3390/proceedings2024110014

García, D., Díaz, J., Martín, A., and Cobos, E., 2022: Spatiotemporal Analysis of Urban Thermal Effects Caused by Heat Waves through Remote Sensing. *Sustainability*. https://doi.org/10.3390/su141912262.

Gobierno del Estado de Nuevo León. (2024, December 3). Nl.gob.mx. https://nl.gob.mx/es

González-Hernández, D., Meijles, E., and Vanclay, F., 2019: Factors that Influence Climate Change Mitigation and Adaptation Action: A Household Study in the Nuevo Leon Region, Mexico. *Climate*. https://doi.org/10.3390/CLI7060074

Hadi, S.J., Tombul, M., 2018: Comparison of Spatial Interpolation Methods of Precipitation and Temperature Using Multiple Integration Periods. *J Indian Soc Remote Sens* 46, 1187–1199. https://doi.org/10.1007/s12524-018-0783-1

Helbling, M., Meierrieks, D., 2018: Global warming and urbanization. J Popul Econ 36, 1187–1223. https://doi.org/10.1007/s00148-022-00924-y

Hu, Y., Jia, G., Gao, H., Li, Y., Hou, M., Li, J., and Miao, C. (2023). Spatial characterization of global heat waves using satellite-based land surface temperature. Int. J. Appl. Earth Obs. Geoinformation, 125, 103604. https://doi.org/10.1016/j.jag.2023.103604.

Kamath, H., Martilli, A., Sigh M., Brooks, T., Lanza, K., Bixler, R. P., Coudert, M., Yang, Z-L., Niyogi, D. (2023). Human heat health index (H3I) for holistic assessment of heat hazard and mitigation strategies beyond urban heat islands. Urban Climate, 52, https://doi.org/10.1016/j.uclim.2023.101675

Karakaya Aytin, Beste and Ertin Tezgör, Deniz and Özyavuz, Murat. (2016). Environmental Noise Pollution in The City of Edirne - Turkey.

Lanzante, J., 2024: A New Heat Stress Index For Climate Change Assessment. *Bulletin of the American Meteorological Society*. https://doi.org/10.1175/bams-d-24-0030.1

Liu, M., Li, X., Chai, Z., Chen, A., Zhang, Y., and Zhang, Q., 2023: Dense Temperature Mapping and Heat Wave Risk Analysis Based on Multisource Remote Sensing Data. *IEEE Journal of Selected Topics in Applied Earth Observations and Remote Sensing*, 16, 3148-3157. https://doi.org/10.1109/JSTARS.2023.3260467.

Lu, G., and Wong, D. (2008). An adaptive inverse-distance weighting spatial interpolation technique. Comput. Geosci., 34, 1044-1055. https://doi.org/10.1016/j.cageo.2007.07.010.

Lucia, F.-M. A., and Ulises, R.-S. H., 2023: Evolution of Air Pollution in the Monterrey Metropolitan Area, Mexico. *Asian Journal of Environment and Ecology*, 21(1), 55–75. https://doi.org/10.9734/ajee/2023/v21i11453

Magaña, V., Herrera, E., Ábrego-Góngora, C., and Avalos, J., 2021: Socioeconomic Drought in a Mexican Semi-arid City:

Monterrey Metropolitan Area, a Case Study., 3. https://doi.org/10.3389/frwa.2021.579564.

Mayora, F., 2020: Contaminación del aire en Monterrey, Nuevo León: interpretación del monitoreo ambiental 2005-2018. *REVISTAS DE INVESTIGACIÓN*, 43(98).

Ozelkan, E., Bagis, S., Ozelkan, E. C., Ustundag, B. B., Yucel, M., and Ormeci, C., 2015. Spatial interpolation of climatic variables using land surface temperature and modified inverse distance weighting. *International Journal of Remote Sensing*, 36(4), 1000–1025. https://doi.org/10.1080/01431161.2015.1007248

Qiao, P., Lei, M., Yang, S. et al., 2018: Comparing ordinary kriging and inverse distance weighting for soil as pollution in Beijing. *Environ Sci Pollut Res* 25, 15597–15608. https://doi.org/10.1007/s11356-018-1552-y

Rachid, A., and Qureshi, A. (2023). Sensitivity Analysis of Heat Stress Indices. *Climate*. https://doi.org/10.3390/cli11090181.

Romps, D., and Lu, Y., 2023: The Heat Index as a Measure of Future Heat Stress with Climate Change. Physiology. https://doi.org/10.1152/physiol.2023.38.s1.5734222.

Servicio Meteorológico Nacional. (n.d.). smn.conagua.gob.mx. https://smn.conagua.gob.mx/es/

Shi, H., Xian, G., Auch, R., Gallo, K., and Zhou, Q., 2021: Urban Heat Island and Its Regional Impacts Using Remotely Sensed Thermal Data—A Review of Recent Developments and Methodology. *Land*. https://doi.org/10.3390/land10080867.

Silberstein, M., 2024: Global warming is intensifying due to population growth and food production. *Research Square*. https://doi.org/10.21203/rs.3.rs-4423590/v1

Szymanowski, M., Kryza, M. (2009) GIS-bsed techniques for urban heat island spatialization. Clim Res 38:171-187 https://doi.org/10.3354/cr00780

Tian, L., Lu, J., Li, Y. C., Bu, D., Liao, Y., and Wang, J., 2021: Temporal characteristics of urban heat island and its response to heat waves and energy consumption in the mountainous Chongqing, China. *Sustain. Cities Soc.* 75:103260. doi: 10.1016/j.scs.2021.103260

Tian, W., Yang, Y., Wang, L., Zong, L., Zhang, Y., and Liu, D., 2023: Role of local climate zones and urban ventilation in canopy urban heat island–heatwave interaction in Nanjing megacity, China. *Urban Climate*, 49, 101474.https://doi.org/10.1016/j.uclim.2023.101474

US Department of Commerce, N., 2024: What is the heat index? Www.weather.gov. https://www.weather.gov/ama/heatindex

Vivideconomics, 2022: Extreme Heat: The Economic and Social Consequences for Global Cities. https://onebillionresilient.org/wp-content/uploads/sites/2/2022/09/Hot-Cities-Chilled-Economies-Public-Methodology.pdf

Willmott, C. J., & Matsuura, K. 2005: *Advantages of the mean absolute error (MAE) over the root mean square error (RMSE) in assessing average model performance*. Climate Research. 30(1), 79–82. http://www.jstor.org/stable/24869236

Xu, C., Wei, R., and Tong, H. (2025). A Systematic Review of Methodological Advances in Urban Heatwave Risk Assessment: Integrating Multi-Source Data and Hybrid Weighting Methods. Sustainability, 17(8), 3747. https://doi.org/10.3390/su17083747

Zapata Wah, I. G., Yépez Rincón, F. D., and Velastegui-Montoya, A.: Spatiotemporal Heat Index Assessment in the Monterrey Metropolitan Area during Heat Wave occurrence, ISPRS Ann. Photogramm. Remote Sens. Spatial Inf. Sci., X-3/W3-2025, 165–172, https://doi.org/10.5194/isprs-annals-X-3-W3-2025-165-2026, 2026.